Analytic spatial and temporal temperature profile in a finite laser rod with input laser pulses

Jinho Lee[1,*] and David H. Reitze[1,2]

[1]*Physics Department, University of Florida, Gainesville, Florida 32611, USA*
[2]*LIGO Laboratory, California Institute of Technology, Pasadena, California 91125, USA*
[*]*kjindda@naver.com*

Abstract: In this communication, we present an analytic expression of the thermal load in a cylindrical laser rod. We consider a pump beam with Gaussian temporal and spatial profile, which permits, using superposition of the single pulse solution, an explicit calculation of the optical path length difference across the radial direction of the rod and of the transient thermal focal length changes for a variable pump repetition rate and pulse width. We have chosen to model Ti:Al_2O_3 as a specific example, however our solution is completely general and can be applied to any materials with cylindrical geometry employing a stable laser cavity design.

OCIS codes: (140.6810) Thermal effects; (140.3280) Laser amplifiers; (140.3425) Laser stabilization.

References and links

1. V. Ramanathan, J. Lee, S. Xu, X. Wang, L. Williams, W. Malphurs, and D. H. Reitze, "Analysis of thermal aberrations in a high average power single-stage Ti:sapphire regenerative chirped pulse amplifier: Simulation and experiment," Rev. Sci. Instrum. **77**(10), 103103 (2006).
2. F. Salin, C. L. Blanc, J. Squier, and C. Barty, "Thermal eigenmode amplifiers for diffraction-limited amplification of ultrashort pulses," Opt. Lett. **23**(9), 718–720 (1998).
3. W. Koechner, *Solid-State Laser Engineering* (Springer-Verlag, 1988), Chap. 7.
4. R. Weber, B. Neuenschwander, M. Mac Donald, M. B. Roos, and H. P. Weber, "Cooling schemes for longitudinally diode laser-pumped Nd:YAG rods," IEEE J. Quantum Electron. **34**(6), 1046–1053 (1998).
5. R. Lausten and P. Balling, "Thermal lensing in pulsed laser amplifiers: an analytical model," J. Opt. Soc. Am. B **20**(7), 1479–1485 (2003).
6. U. O. Farrukh, A. M. Buoncristiani, and C. E. Byvik, "An analysis of the temperature distribution in finite solid-state saser rods," IEEE J. Quantum Electron. **24**(11), 2253–2263 (1988).
7. H. S. Carslaw and J. C. Jaeger, *Conduction of heat in solids* (Oxford Univ., 1948), pp. 191.
8. P. F. Moulton, "Spectroscopic and laser characteristics of Ti:Al_2O_3," J. Opt. Soc. Am. B **3**(1), 125–133 (1986).
9. M. L. Boas, *Mathematical Methods in the Physical Sciences* (John Wiley & Sons, 1993).
10. J. D. Jackson, *Classical Electrodynamics* (John Wiley & Sons, 1998), Chap. 4.
11. G. N. Watson, *Theory of Bessel Functions* 2nd edition (Cambridge University, 1922), pp. 393.
12. P. A. Schulz and S. R. Henion, "Liquid-nitrogen-cooled Ti:Al_2O_3 laser," IEEE J. Quantum Electron. **27**(4), 1039–1047 (1991).
13. E. Wyss, M. Roth, T. Graf, and H. P. Weber, "Thermooptical compensation methods for high-power lasers, "IEEE," Quantum Electron. **38**(12), 1620–1628 (2002).

Over the past twenty years, the development of high-repetition, high average power amplifier of solid-state laser materials has revived considerable interest in optically pumped solid-state lasers [1–13]. However, the energy deposited to excite the gain media generates a dynamic heating profile in the material, resulting in a spatial-dependent refractive index. Since the refractive index in a laser material is temperature dependent, the gain material exhibits a spatial index variation, resulting in potentially severe focusing of the seed laser (thermal lensing). Different solutions to this problem have emerged, including the introduction of compensating optics in the amplifier [2] and an amplifier design based on a cryogenically cooled crystal (since thermal conductivity of Ti:Al_2O_3 increases with decreasing temperature) [1].

#227056 - $15.00 USD Received 19 Nov 2014; revised 17 Jan 2015; accepted 19 Jan 2015; published 29 Jan 2015

Since Koechner pioneered this field (see [3] and references herein), a number of analytic solutions for the thermal lensing properties have been presented [4–7]. For example, the general solution for describing the thermal profile in an "infinite" cylinder is given by [7]. However, to our knowledge none of these analyses has solved the exact analytic thermal expression in a finite cylindrical geometry including a transient temperature profile for Gaussian spatial profile and time profile based on the input pulses. This is important because the high heat intensity of such a powerful laser can be used to calculate thermal lensing distortions and beam mode changes in all optical components.

Here, an analytic expression is presented for thermal lensing properties of optical crystals with Gaussian spatial and temporal profile of the source term. The fully analytic expression given in this paper can also be used to establish a stable laser cavity. We focus on the thermal load in Ti:Al_2O_3 because it is proven material for high-power laser applications [8], but our solution is general and can be applied to any kind of materials with cylindrical geometry.

In this paper, we consider the case in which the pump light absorption generates the heat within the laser rod; this heat is removed by a coolant flowing only along the cylindrical rod surface. The heat loss from the free ends of the crystal is neglected [5,6]. With this assumption, the heat flows radially and also longitudinally. For the calculation of the temperature distribution in a laser material, we assume that physical properties of the material (thermal conductivity, absorption coefficient and so forth) are constant over the range of temperatures involved in the heat equation and that the heat transport within the material is isotropic [6]. Based on these assumptions, we start our analysis from the classical heat equation, specifying the time evolution of the temperature at all points in a laser load [5,6]

$$C\frac{\partial T}{\partial t} - \kappa \nabla^2 T = S(r,t) \tag{1}$$

where C and κ are the laser material's heat capacity and its thermal conductivity. $S(r,T)$ represents the thermal power density of the thermal heat source and can be expressed as a Gaussian spatial time profile of a pulse in case of a single pulse operation,

$$S(r,t) = Ne^{-2\frac{r^2}{\omega^2}} e^{-\alpha z} e^{-2\frac{(t-\Delta t)^2}{\tau_h^2}} \tag{2}$$

where N, 2ω, $2\tau_h$ and Δt are the normalization factor, a beam diameter, a pulse width, and the temporal center of the Gaussian, respectively. Since S is the power density, i.e. energy per unit time and unit volume, the integration with respect to space (when l is the length of the laser rod) and time is the heat dissipated in the laser rod from a single pulse energy, A:

$$\int_{-\infty}^{\infty}\int_{0}^{l}\int_{-\infty}^{\infty}\int_{-\infty}^{\infty} Ne^{-2\frac{r^2}{\omega^2}} e^{-\alpha z} e^{-2\frac{(t-\Delta t)^2}{\tau_h^2}} dxdydzdt = N\frac{\omega^2\pi}{2}\frac{1-e^{-\alpha l}}{\alpha}\sqrt{\frac{\pi}{2}}\tau_h = A \tag{3}$$

$$N = \frac{2A}{\pi\omega^2\tau_h}\frac{\alpha}{1-e^{-\alpha l}}\sqrt{\frac{2}{\pi}} \tag{4}$$

In most end-pumped laser cavity, the time varying source term is a linear sum of multiple Gaussians:

$$\begin{aligned} S(r,t) &= \frac{2A}{\pi\omega^2\tau_h}\frac{\alpha}{1-e^{-\alpha l}}\sqrt{\frac{2}{\pi}} e^{-2\frac{r^2}{\omega^2}} e^{-\alpha z}\left[e^{-2\frac{(t-\Delta t)^2}{\tau_h^2}} + e^{-2\frac{(t-2\Delta t)^2}{\tau_h^2}} + e^{-2\frac{(t-3\Delta t)^2}{\tau_h^2}} + e^{-2\frac{(t-4\Delta t)^2}{\tau_h^2}} \cdots \right] \\ &= \frac{2A}{\pi\omega^2\tau_h}\frac{\alpha}{1-e^{-\alpha l}}\sqrt{\frac{2}{\pi}} e^{-2\frac{r^2}{\omega^2}} e^{-\alpha z}\sum_{q=1}^{\infty} e^{-2\frac{(t-q\Delta t)^2}{\tau_h^2}} \end{aligned} \tag{5}$$

#227056 - $15.00 USD Received 19 Nov 2014; revised 17 Jan 2015; accepted 19 Jan 2015; published 29 Jan 2015

Given a geometry in laser materials of cylindrical symmetry with radius a and length l, several boundary conditions could be imposed [6]. For the case of an end-pumped crystal in thermal contact with a liquid-cooled holder, constant temperature at the cylindrical surface is an appropriate boundary condition. Neglecting heat loss from the free ends of the crystal, the derivative of the solution vanishes at the end points [5,6].

$$T(r=a,z,t)=\text{Constant} \tag{6}$$

$$\left.\frac{dT}{dz}\right|_{z=0,l}=0 \tag{7}$$

For the system of cylindrical symmetry, Eq. (1) takes the form

$$C\frac{\partial T(r,z,t)}{\partial t}-\kappa\left(\frac{\partial^2}{\partial r^2}+\frac{1}{r}\frac{\partial}{\partial r}+\frac{\partial^2}{\partial z^2}\right)T(r,z,t)=\frac{2A}{\pi\omega^2\tau_h}\frac{\alpha}{1-e^{-\alpha l}}\sqrt{\frac{2}{\pi}}e^{-2\frac{r^2}{\omega^2}}e^{-\alpha z}\,e^{-2\frac{(t-\Delta t)^2}{\tau_h^2}} \tag{8}$$

With the form of a single pulse operation as shown in Eq. (8), the general solution can be directly obtained by using the method of separating variables [9]. Bessel functions of the first kind $J_0(k_n\frac{r}{a})$ satisfying [9,10]

$$\frac{1}{r}\frac{d}{dr}[r\frac{dJ_0(k_n\frac{r}{a})}{dr}]+\frac{k_n^2}{a^2}J_0(k_n\frac{r}{a})=0 \tag{9}$$

and orthogonal condition [9,10]

$$\int_0^a rJ_0(k_n\frac{r}{a})J_0(k_m\frac{r}{a})dr=\frac{a^2}{2}J_1(k_n)^2\delta_{nm}=\frac{a^2}{2}J_0(k_n)'^2\delta_{nm} \tag{10}$$

form an orthogonal complete set of functions, and the general solution of Eq. (8) becomes

$$T(r,z,t)=\sum_{m=0}^{\infty}\sum_{n=1}^{\infty}A_nJ_0(k_n\frac{r}{a})[B_m\cos(l_mz)+C_m\sin(l_mz)]\varphi_{nm}(t) \tag{11}$$

The boundary condition (Eq. (7)) results only in a z-dependent cosine series ($C_m=0$) and $l_m=\frac{m\pi}{l}$ (where $m=0\ldots\infty$).

Inserting Eq. (11) into Eq. (8) and using Eq. (9) leads to

$$\begin{aligned}&C\frac{\partial T(r,z,t)}{\partial t}-\kappa\nabla^2T(r,z,t)\\&=\sum_{n=1}^{\infty}A_nJ_0(k_n\frac{r}{a})\sum_{m=0}^{\infty}B_m\cos(\frac{m\pi}{l}z)\,(C\frac{d\varphi_{nm}(t)}{dt}+\kappa\frac{k_n^2}{a^2}\varphi_{nm}(t)+\kappa(\frac{m\pi}{l})^2\varphi_{nm}(t))\\&=\frac{2A}{\pi\omega^2\tau_h}\frac{\alpha}{1-e^{-\alpha l}}\sqrt{\frac{2}{\pi}}e^{-2\frac{r^2}{\omega^2}}e^{-\alpha z}\;e^{-2\frac{(t-\Delta t)^2}{\tau_h^2}}\end{aligned} \tag{12}$$

#227056 - $15.00 USD Received 19 Nov 2014; revised 17 Jan 2015; accepted 19 Jan 2015; published 29 Jan 2015

Since $e^{-2\frac{r^2}{\omega^2}}$ can be expanded with Bessel functions $e^{-2\frac{r^2}{\omega^2}} = \sum_{n=1}^{\infty} C_n J_0(k_n \frac{r}{a})$, we multiply this equation by $rJ_0(k_m \frac{r}{a})$, integrate from 0 to a and use the orthogonality conditions of the Bessel functions (Eq. (10)) to obtain

$$\begin{aligned} e^{-2\frac{r^2}{\omega^2}} &= \sum_{n=1}^{\infty} C_n J_0(k_n \frac{r}{a}) \\ C_n &= \frac{2}{a^2 J_1(k_n)^2} \int_0^a e^{-2\frac{r^2}{\omega^2}} r J_0(k_n \frac{r}{a}) dr \end{aligned} \tag{13}$$

Using the fact that (in most cases) the beam waist ω is smaller than the radius of the laser rod and an oscillation of the Bessel function $J_0(k_m \frac{r}{a})$ decays as r increases, we could approximate the integration in Eq. (13) from 0 to infinite. With $\int_0^{\infty} J_0(at) e^{-p^2 t^2} t dt = \frac{1}{2p^2} e^{-\frac{a^2}{4p^2}}$ from [11], the coefficient C_n can be simplified as

$$C_n \approx \frac{\omega^2}{2a^2 J_1(k_n)^2} e^{-\frac{\omega^2 k_n^2}{8a^2}} \tag{14}$$

Similarly, $e^{-\alpha z}$ can be expanded with cosine series $e^{-\alpha z} = \sum_{m=0}^{\infty} D_m \cos(\frac{m\pi}{l} z)$. If we multiply this equation by $\cos(\frac{n\pi}{l} z)$, integrate from 0 to l and use the orthogonality conditions of the cosine functions,

$$\begin{aligned} \int_0^l \cos(\frac{m\pi}{l} z) \cos(\frac{n\pi}{l} z) dz &= \frac{l}{2} \delta_{mn} \quad m = n \neq 0, \\ &= l \delta_{0n} \quad m = n = 0 \end{aligned}$$

we get

$$e^{-\alpha z} = \sum_{m=0}^{\infty} D_m \cos(\frac{m\pi}{l} z) \tag{15}$$

where

$$\begin{aligned} D_0 &= -\frac{e^{-\alpha l} - 1}{\alpha l} \\ D_m &= -\frac{2(\cos(m\pi) e^{-\alpha l} - 1)}{\alpha l (1 + (\frac{m\pi}{\alpha l})^2)} \end{aligned}$$

Inserting these two expressions (Eqs. (13) and (15)) into Eq. (12), we find

$$A_n = \frac{2A}{\pi \omega^2 \tau_h} \frac{\alpha}{1 - e^{-\alpha l}} C_n \tag{16}$$

#227056 - $15.00 USD Received 19 Nov 2014; revised 17 Jan 2015; accepted 19 Jan 2015; published 29 Jan 2015

$$B_n = D_n \tag{17}$$

$$(C\frac{d\varphi_{mn}(t)}{dt} + \kappa\frac{k_n^2}{a^2}\varphi_{mn}(t) + \kappa(\frac{m\pi}{l})^2\varphi_{mn}(t)) = \sqrt{\frac{2}{\pi}}e^{-2\frac{(t-\Delta t)^2}{\tau_h^2}} \tag{18}$$

We have obtained the coefficients for spatial components of the general solution, Eq. (11). To obtain the complete solution, including transient heat conduction in the finite rod, we need to solve Eq. (18). Setting $\kappa\frac{k_n^2}{a^2} + \kappa(\frac{m\pi}{l})^2 \equiv \kappa_{nm}$, Eq. (18) leads to

$$C\frac{d\varphi_{nm}(t)}{dt} + \kappa_{nm}\varphi_{nm}(t) = \sqrt{\frac{2}{\pi}}e^{-2\frac{(t-\Delta t)^2}{\tau_h^2}} \tag{19}$$

Multiplying $e^{\frac{\kappa_{nm}}{C}t}$ by both sides of Eq. (19), the equation can be expressed as

$$\frac{de^{\frac{\kappa_{nm}}{C}t}\varphi_{nm}(t)}{dt} = \frac{e^{\frac{\kappa_{nm}}{C}t}}{C}\sqrt{\frac{2}{\pi}}e^{-2\frac{(t-\Delta t)^2}{\tau_h^2}} \tag{20}$$

Therefore the time-dependent solution $\varphi_{nm}(t)$ leads to

$$\varphi_{nm}(t) = e^{-\frac{\kappa_{nm}}{C}t}\frac{1}{C}\sqrt{\frac{2}{\pi}}\int_{t=-\infty}^{t=t}[e^{\frac{\kappa_{nm}}{C}t}e^{-2\frac{(t-\Delta t)^2}{\tau_h^2}}]dt \tag{21}$$

with the condition $\varphi_{nm}(-\infty) = 0$.

Since $\frac{\kappa_{nm}}{C}t - 2\frac{(t-\Delta t)^2}{\tau_h^2} = -\frac{2}{\tau_h^2}(t - \frac{\tau_h^2}{4}(\frac{\kappa_{nm}}{C} + \frac{4\Delta t}{\tau_h^2}))^2 + \frac{\tau_h^2}{8}(\frac{\kappa_{nm}}{C} + \frac{4\Delta t}{\tau_h^2})^2 - \frac{2\Delta t^2}{\tau_h^2}$,

Equation (21) takes the form

$$\varphi_{nm}(t) = \frac{e^{-\frac{\kappa_{nm}}{C}t}}{C}\sqrt{\frac{2}{\pi}}e^{\frac{\tau_h^2}{8}(\frac{\kappa_{nm}}{C}+\frac{4\Delta t}{\tau_h^2})^2 - \frac{2\Delta t^2}{\tau_h^2}}\int_{t=-\infty}^{t=t}[e^{-\frac{2}{\tau_h^2}(t-\frac{\tau_h^2}{4}(\frac{\kappa_{nm}}{C}+\frac{4\Delta t}{\tau_h^2}))^2}]dt \tag{22}$$

With substitution of $t' \equiv \frac{\sqrt{2}}{\tau_h}(t - \frac{\tau_h^2}{4}(\frac{\kappa_{nm}}{C} + \frac{4\Delta t}{\tau_h^2}))$

$$\varphi_{nm}(t) = \frac{\tau_h}{C\sqrt{\pi}}e^{-\frac{\kappa_{nm}}{C}t}e^{\frac{\tau_h^2}{8}(\frac{\kappa_{nm}}{C}+\frac{4\Delta t}{\tau_h^2})^2 - \frac{2\Delta t^2}{\tau_h^2}}\int_{t'=-\infty}^{t'=\frac{\sqrt{2}}{\tau_h}(t-\frac{\tau_h^2}{4}(\frac{\kappa_{nm}}{C}+\frac{4\Delta t}{\tau_h^2}))}e^{-t'^2}dt. \tag{23}$$

The form of integration is a simple error function defined in [9] as

$$erf(t) = \frac{2}{\sqrt{\pi}}\int_0^t e^{-t^2}dt$$

Therefore, the time-dependent solution can be expressed as

$$\varphi_{nm}(t) = \frac{\tau_h}{2C}e^{-\frac{\kappa_{nm}}{C}t}e^{\frac{\tau_h^2}{8}(\frac{\kappa_{nm}}{C}+\frac{4\Delta t}{\tau_h^2})^2 - \frac{2\Delta t^2}{\tau_h^2}}[(1-\theta(t'))(1-erf(-t')) + \theta(t')(1+erf(t'))] \tag{24}$$

where $\theta(t') = 0 \quad (or\ 1)$ when $t' < 0$ (or $t' \geq 0$)

We thus have the full solution-satisfying Eq. (8)

#227056 - $15.00 USD Received 19 Nov 2014; revised 17 Jan 2015; accepted 19 Jan 2015; published 29 Jan 2015

$$T(r,z,t)=\sum_{m=0}^{\infty}\sum_{n=1}^{\infty}A_n J_0(k_n\frac{r}{a})B_m\cos(\frac{m\pi}{l}z)\varphi_{nm}(t)$$

$$A_n=\frac{2A}{\pi\omega^2\tau_h}\frac{\alpha}{1-e^{-\alpha l}}C_n$$

$$B_n=D_n$$

$$\varphi_{nm}(t)=\frac{\tau_h}{2C}e^{-\frac{\kappa_{nm}}{C}t}e^{\frac{\tau_h^2}{8}(\frac{\kappa_{nm}}{C}+\frac{4\Delta t}{\tau_h^2})^2-\frac{2\Delta t^2}{\tau_h^2}}[(1-\theta(t'))(1-erf(-t'))+\theta(t')(1+erf(t'))]$$

If a laser rod is pumped by a single pulse, a transient thermal profile will be established as a result of the fast heating process followed by a slow recovery of the rod to thermal equilibrium as shown in Fig. 1(a) with the boundary condition $T(r = a,z) = 0$ corresponding a fixed surface temperature, which is taken as zero since the heat transport equation is linear.

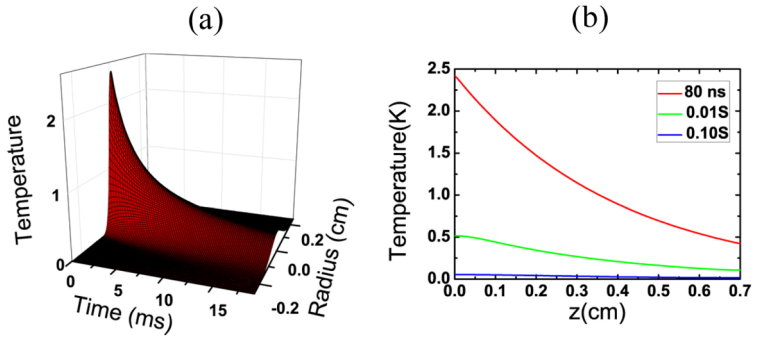

Fig. 1. (a) Thermal relaxation of the laser rod of a single input pulse in a cylindrical geometry (0.7-cm long, 0.25-cm radius). For this calculation, we used a time duration, $\tau = 160ns$ and a pulse energy of $10mJ$. (b) Longitudinal temperature distribution shows the initial exponential (rd curve) and temperature distribution at various times at $r = 0$.

As illustrated in Fig. 1(a), temperature increases without any observable delay with respected to the energy deposited in the rod. The longitudinal temperature evolution is plotted in Fig. 2(b) at varying times. The thermal conductivity, heat capacity, and absorption coefficient applied are $\kappa = 0.33Wcm^{-1}K^{-1}$, $C = 3.1Jcm^{-3}K^{-1}$, and $\alpha = 2.5/cm$ [12], corresponding to the values when pumping at 532 nm of Ti:sapphire crystal with 0.15 doping. We assumed the input beam radius as 50 μm.

We now allow the solution $T(r,z,t)$ to evolve to increase the crystal temperature with multiple Gaussian pulses. As seen from Eq. (5), multiple Gaussian pulses can be involved to increase the crystal temperature. Since $\varphi_{nm}(t)$ is the solution of the differential Eq. (24) with one Gaussian pulse input, $\sqrt{\frac{2}{\pi}}e^{-2\frac{(t-\Delta t)^2}{\tau_h^2}}$, the time-dependent solution for many input pulses can be expressed as

$$\varphi_{mn}(t)\big|_{general}=\varphi_{mn}(t)+\varphi_{mn}(t-\Delta t)+\varphi_{mn}(t-2\Delta t)+\cdots=\sum_{q=0}^{\infty}\varphi_{mn}(t-q\Delta t) \qquad (25)$$

Therefore the solution of a single-shot operation can be used for multiple Gaussian inputs. Figure 2 shows a thermal build-up when multiple pulses are introduced to the laser rod with a pulse interval that is smaller than the thermal relaxation time. Under these conditions, a steady-state operating condition will soon be established by the laser (as shown in Fig. 2(b))

#227056 - $15.00 USD Received 19 Nov 2014; revised 17 Jan 2015; accepted 19 Jan 2015; published 29 Jan 2015

in which the radial flow of heat out of the rod equals the total heat being put into the rod. In the extreme case, when the pulse interval time becomes negligibly small as compared to the thermal relaxation time, the transient thermal profile in the laser rod approaches the continuous wave condition. In this region, thermal effects depend only on the average input power.

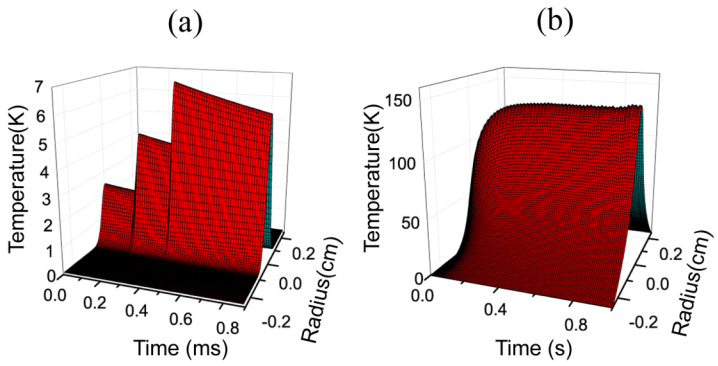

Fig. 2. Thermal buildup when the pulse interval time is less than the thermal relaxation time. For the calculation: (a) three respectively pulsed lasers are introduced to the laser rod with 20μs pulse separation; (b) five thousand pulsed lasers are introduced to the laser with 5-kHz repetition rate. All parameters for the calculation are the same as those given for Fig. 1.

The transient temperature distribution in a laser rod as illustrated in Fig. 2 eventually affects energy output and beam divergence of the laser. The transient thermal lensing properties of a seed pulse sent through the amplifier samples depends on the optical path length of the seed pulse through the crystal and simply takes the form

$$l(r,t)=\int_{z=0}^{l} n(T(r,z,t))dz \tag{26}$$

The refractive index near the center of the crystal can be approximated by a first-order expansion around the temperature of the center, T_C [5]

$$n(T)\approx n(T_C)+\left.\frac{\partial n}{\partial T}\right|_{T_C}(T-T_C) \tag{27}$$

$$\Delta l(r,t)=\left.\frac{\partial n}{\partial T}\right|_{T_C}\int_{z=0}^{l}[T(r,z,t)-T(r=0,z,t)]dz \tag{28}$$

As shown in [5], the z-dependent thermal profile contains $\cos(\frac{m\pi}{l})$ and vanishes after integration along z except for an $m = 0$ constant term

$$\int_{z=0}^{l} T(r,z,t)dz=\sum_{n=1}^{\infty}A_n J_0(k_n\frac{r}{a})\frac{1-e^{-\alpha l}}{\alpha}\varphi_{n0}(t) \tag{29}$$

Using a zero-order Bessel function around $r = 0$, $J_0(k_n\frac{r}{a})\approx 1-(\frac{k_n r}{2a})^2$ when $k_n\frac{r}{a}<<1$ [9] and Eq. (14) for the case of $\omega << a$

#227056 - $15.00 USD Received 19 Nov 2014; revised 17 Jan 2015; accepted 19 Jan 2015; published 29 Jan 2015

$$\Delta l(r,t) \approx \left.\frac{\partial n}{\partial T}\right|_{T_C} \sum_{n=1}^{\infty} A_n((1-(\frac{k_n r}{2a})^2 - J_0(0))\frac{1-e^{-\alpha l}}{\alpha}\varphi_{n0}(t))$$

$$= -r^2 \left.\frac{\partial n}{\partial T}\right|_{T_C} \sum_{n=1}^{\infty} \frac{\alpha A}{(1-e^{-\alpha l})a^2 \pi \tau_h J_1(k_n)^2} e^{-\frac{\omega^2 k_n^2}{8a^2}} (\frac{k_n}{2a})^2 \frac{1-e^{-\alpha l}}{\alpha}\varphi_{n0}(t) \qquad (30)$$

$$= -r^2 \left.\frac{\partial n}{\partial T}\right|_{T_C} \sum_{n=1}^{\infty} \frac{A k_n^2 e^{-\frac{\omega^2 k_n^2}{8a^2}} \varphi_{n0}(t)}{4a^4 \pi \tau_h J_1(k_n)^2}$$

The Bessel function expansion for $k_n \frac{r}{a} << 1$ is valid because, for the higher k_n value, $e^{-\frac{\omega^2 k_n^2}{8a^2}}$ becomes smaller and total contribution for optical path length difference for higher n (or k_n) vanishes.

A spherical lens of curvature from the quadratic form of the optical path length difference $\Delta l \approx -\frac{r^2}{2R}$ [5] gives a result of $f = \frac{R}{n-1}$ [5]. With this spherical approximation and Eq. (30), the focal length change by thermal load in the laser rod will be

$$f = \frac{1}{\left.\frac{\partial n}{\partial T}\right|_{T_C} \sum_{n=1}^{\infty} \frac{A k_n^2 e^{-\frac{\omega^2 k_n^2}{8a^2}} \varphi_{n0}(t)(n-1)}{2a^4 \pi \tau_h J_1(k_n)^2}} \qquad (31)$$

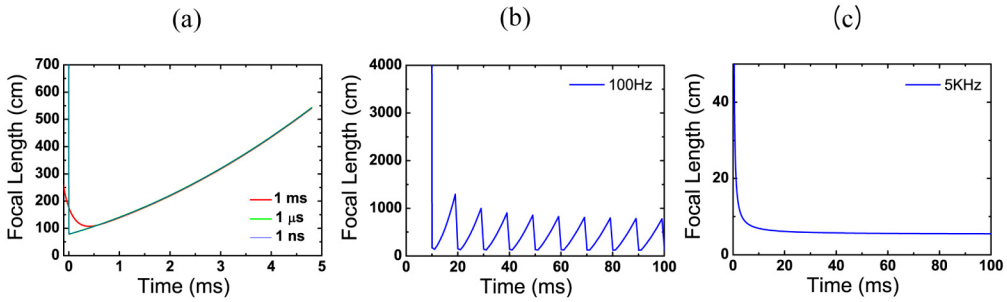

Fig. 3. (a) Transient focal length change of one single pulse for 1 ms (solid red), 1 μs (solid green) and 1 *ns* (solid blue) time duration. Focal length changes of (b) 100 Hz and (c) 5 kHz repetitively pulsed pump laser input for a 1*ms,* 10*mJ* pulse. All of the parameters used in this calculation except for the pulse duration and the repetition rate are equal for all three cases and identical to those used in Fig. 1.

Figure 3(a) shows the transient focal length change for a single pulse operation. There is a focal length difference between a 1-ms pulse and 1 μs at earlier time region comparable with the pulse widths shown in Fig. 3(a). However, since temperature increases without any observable delay with respected to the energy deposited in the rod for a pulse lasting from 1 *ns* to 1μs (as seen from Fig. 3(a)), we found that the transient focal length shows negligible dependency on the pulse width with a pulse lasting for between 1*ns* to 1 μs. The transient focal length changes for all these three cases follows the same line after 1 ms. For multiple pulse input, when the time separation between pulses is comparable to the material's thermal relaxation time, we have a result of transient focal length variation as shown in Fig. 3(b) as we could expect, and it never becomes stable (it varies between 20 and 1000 cm in Fig. 3(b)). However, with a high enough pulse repetition rate as shown in Fig. 3(c), the focal length

#227056 - $15.00 USD Received 19 Nov 2014; revised 17 Jan 2015; accepted 19 Jan 2015; published 29 Jan 2015

become steady and the focal length at the final steady state is less than 5 cm. Due to the simplicity of the focal length expression (Eq. (31)), it is well suited for the evaluation of the acceptable parameter range for future solid-state laser cavity (by analyzing this thermo-optical property of the system, it is possible to estimate the minimum repetition rate of pump laser to give a stable laser cavity design).

All of these types of transient focal length changes in the laser cavity result in serious seed beam distortion through the laser rod, making the establishment of either a high (or low) repetition rate for stable unamplified laser activity impossible. However, thermally induced beam distortion can successfully be removed with the self-adaptive optical elements [13] as described at the beginning of this paper. Placing a suitable material having negative dn/dT after the laser rod, self-balancing thermal lenses can be developed [13]. Appropriate design of the compensation devices can be obtained by the above thermal analysis.

In summary, we provide the exact analytic expression, including the transient temperature profile, for a laser-pumped solid-state amplified system. The analysis can directly be applied for the evaluation of thermal-lensing effects for the future development of laser technologies. Since the calculation in this paper assumes that all pulse energy is deposited as heating of the crystal rod, the results presented here are the upper limits of the thermal effects.

#227056 - $15.00 USD Received 19 Nov 2014; revised 17 Jan 2015; accepted 19 Jan 2015; published 29 Jan 2015